Acta Mechanica Solida Sinica (2024) 37:598–612
https://doi.org/10.1007/s10338-023-00459-z

Surface Elastic Effects on Electromechanical Responses of a Piezoelectric Semiconducting Nanobeam

Aowen Bao[1] · Xiaobao Li[1] · Yuxue Pu[1] · Chunxiao Zhan[1]

Received: 8 October 2023 / Revised: 16 December 2023 / Accepted: 19 December 2023 / Published online: 7 February 2024

Abstract
Piezoelectric semiconductors (PSCs) find extensive applications in modern smart electronic devices because of their dual properties of being piezoelectric and semiconductive. With the increasing demand for miniaturization of these devices, the performance of their components needs to be carefully designed and optimized, especially when reduced to nanosize. It has been shown that surface elastic properties play a substantial role in the mechanical performance of nanoscale materials and structures. Building on this understanding, the surface elastic effects, encompassing surface residual stress, surface membrane stiffness, and surface bending stiffness, are comprehensively taken into account to explore the electromechanical responses of a PSC nanobeam. Additionally, the flexoelectric effect on their responses is also systematically studied. The results of this work reveal that surface elastic properties predominantly influence mechanical performance, while the flexoelectric effect plays a more dominant role in electric-related quantities at the nanoscale. Notably, the significance of surface bending rigidity, which was often underestimated in the earlier literature, is demonstrated. Furthermore, owing to the flexoelectric effect, the linear distribution of electric potential and charge carriers along the length transforms into a nonlinear pattern. The distributions of electric potential and charge carriers across the cross section are also evidently impacted. Moreover, the size-dependent responses are evaluated. Our findings may provide valuable insights for optimizing electronic devices based on nanoscale PSCs.

Keywords Surface elastic effect · Flexoelectricity · Size effect · Piezoelectric semiconductor

1 Introduction

Piezoelectric semiconductors (PSCs) have garnered widespread use in multi-functional and intelligent electronic devices due to their possession of both piezoelectric and semiconductive properties [1]. In PSCs, a mechanical force may stimulate polarizations/electric fields, leading to a redistribution of their internal charge carriers. Conversely, deformations and motion of charge carriers in PSCs can also be manipulated by an external voltage. It is such a dual property that endows PSCs with even more fascinating features compared to traditional piezoelectric or semiconducting materials. In recent decades, theoretical studies on these materials have gained growing interest [2]. Particularly, driven by the demands for miniaturization of intelligent electronic devices, a variety of PSC nanostructures have been designed and found numerous applications. Examples include one-dimensional (1D) ZnO nanostructures for energy harvesting [3, 4], acoustic charge transport devices and sensors [5, 6], and others [7–9]. In electronic devices based on PSCs, a key characteristic is the response of charge carriers to external fields such as mechanical stresses. Consequently, numerous studies have focused on the electromechanical behaviors of PSCs under different conditions. It has been reported that stretching and bending deformations can affect the electromechanical responses and motion of charge carriers of the PSC nanowires [10, 11]. Fan et al. showed that carrier redistribution occurs inside the cross section of a bent circular ZnO nanowire when subjected to a static end force, and a smaller initial carrier concentration results in better energy-harvesting efficiency [12]. Additionally, the distribution of charge carriers in a composite beam consisting of piezoelectric dielectric

✉ Xiaobao Li
xiaobaoli@hfut.edu.cn

✉ Yuxue Pu
puyuxue@hfut.edu.cn

[1] School of Civil Engineering, Hefei University of Technology, Hefei 230009, China

and non-piezoelectric semiconductor layers can be tuned through their thickness ratio [13].

In addition to the intrinsic piezoelectricity in PSCs, another novel electromechanical coupling between strain gradient and electrical polarization, named flexoelectricity, has become prominent and also found various applications at the nanoscale [14]. The flexoelectric effect may be manipulated to enhance the intrinsic piezoelectric response [15], e.g., by building piezoelectric/dielectric superlattices. Earlier theoretical work has shown that the flexoelectricity and piezoelectricity are not simply superimposed and can further modify the elastic responses of nanostructures [16]. In fact, the flexoelectricity has been demonstrated to play a more significant role in the electroelastic response of a nanobeam than the piezoelectricity in certain cases [17]. Moreover, flexoelectricity can be triggered in semiconductors, allowing the induced electric potential to tune the distribution of charge carriers. For example, it was found that the motion of charge carriers in composite nanobeams consisting of dielectric and semiconductors can be tuned through the flexoelectric effect alone [18]. It was shown that flexoelectric effect enhances the electric potential of the nanowire, while the semiconducting properties reduce the electric potential [19]. The flexoelectricity and strain gradient have been shown to have noticeable effects on the extension and electronic behaviors of PSC nanowires [20]. Although flexoelectricity is generally induced by strain gradient, the strain gradient itself may have a larger effect than flexoelectricity on the natural frequency and stiffness in the vibration of PSC nanowires [21]. Besides 1D nanostructures, the electromechanical responses of their 2D counterparts, such as flexoelectric semiconducting plates and bilayers, have also been reported [22, 23]. The vibration behaviors and their dependence on the density of charge carriers and the length-to-radius ratio of a PSC plate were studied under the action of biaxial compression and electric potential [24].

It is well known that when the dimensions of materials or structures are reduced to nanoscale, the surface-to-volume ratio increases significantly, leading to considerable surface effects on their mechanical performance. The Gurtin–Murdoch (GM) theoretical framework is often employed to account for surface elastic properties, typically including surface residual stress and surface membrane stiffness, by treating the surface as a deformable membrane with negligible thickness [25, 26]. It has been demonstrated that surface effects can enhance elastic and vibration behaviors [27, 28]. The GM models have been extended to study the mechanical response of piezoelectric nanoplates [29] and ultra-thin films [30]. Distinct from the GM model, Steigmann and Ogden demonstrated the crucial role of curvature-dependent surface energy in the mechanical response of nanostructures by establishing the Steigmann–Ogden (SO) framework [31]. Subsequently, Chhapadia et al. formulated a curvature-dependent surface energy and employed atomistic simulations to demonstrate the effect of surface roughness on bending behaviors of nanostructures [32, 33]. A recent multiscale asymptotic homogenization approach further emphasized the necessity of considering surface bending resistance [34]. Moreover, the effect of surface flexural rigidity on mechanical responses can be significant in elastic medium with embedded spherical inhomogeneity [35] or in contact context [36]. These studies clearly illustrate the importance of surface elastic effect on the elastic performance of nanostructures, particularly the surface bending stiffness for those under compressive or bending loads.

Based on the aforementioned fact that both flexoelectricity and surface elasticity become significant at the nanoscale, a systematic theory has been established to account for them in dielectrics [37]. Liang et al. later simultaneously considered the effects of surface and flexoelectricity on the static bending properties of a dielectric nanobeam [38]. The effects of surface residual stress and surface membrane stiffness on electromechanical bending and vibration behaviors of piezoelectric Timoshenko nanobeams were studied [39]. The impact of both surface and interface energies on the bending deformations of multilayer beams was investigated [40]. The nonlinear free vibration behavior of orthotropic piezoelectric cylindrical nanoshells was reported based on the GM surface energy theory [41]. The flexoelectric and size effects on the static bending and vibration behavior of piezoelectric nanobeams were studied using the GM model [42]. It was found that flexoelectricity always stiffens the elastic behaviors of graphene-based nanobeams, while the surface stress either softens or stiffens depending on its sign [43]. Recent exploration of the surface contributions to flexoelectricity in a finite sample emphasized the necessity of considering the surface effect [44]. Nevertheless, most of these studies have focused on piezoelectric materials, with less attention paid to PSC nanostructures. Recently, Zhang et al. investigated the effects of surface piezoelectricity and surface membrane stiffness on both the static bending and vibration responses of a PSC nanobeam based on the GM theory [45].

Despite these advancements, previous studies primarily focused on surface residual stress and surface membrane stiffness. The importance of surface bending stiffness and flexoelectric effects on the electromechanical behaviors of PSCs has not been adequately addressed, which forms the main motivation for this study. The remainder of this paper is organized as follows: Sect. 2 presents detailed formulations, Sect. 3 presents the electromechanical response of a piezoelectric semiconducting nanobeam considering both surface elastic and flexoelectric effects, and finally, Sect. 4 draws a few conclusions.

2 Theoretical Formulations

The entire theoretical framework for piezoelectric semiconductors is composed of the linear piezoelectricity theory and drift–diffusion theory for semiconductors. The electric Gibbs free energy density for a piezoelectric semiconducting material can be written as

$$U_b = \frac{1}{2}c_{ijkl}\varepsilon_{ij}\varepsilon_{kl} - \frac{1}{2}a_{ij}E_iE_j - e_{kij}E_k\varepsilon_{ij} - f_{ijkl}E_i\eta_{jkl} + \frac{1}{2}g_{ijklmn}\eta_{ijk}\eta_{lmn} \tag{1}$$

where E_i represents the electric potential, ε_{ij} denotes the strain component, η_{jkl} is the strain gradient, c_{ijkl} and g_{ijklmn} are elastic constants and high-order ones, and a_{ij}, e_{kij}, and f_{ijkl} stand for the dielectric, piezoelectric, and flexoelectric coefficients, respectively. The equilibrium equations of motion, together with the charge equation of electrostatics, i.e., Gauss's law involving both doped electrons and holes, are then written as

$$\begin{aligned} &\sigma_{ij,\,j} - \sigma_{ijk,\,jk} + \rho f_i = \rho\ddot{u}_i \\ &D_{i,i} = q(\Delta p - \Delta n) \\ &J^p_{i,i} = -q\frac{\partial \Delta p}{\partial t} \\ &J^n_{i,i} = q\frac{\partial \Delta n}{\partial t} \end{aligned} \tag{2}$$

where u_i and D_i are the displacements and electric displacements, respectively. The remaining physical quantities are the body force components f_i, the elementary charge $q = 1.6 \times 10^{-19}$ C, the hole and electron current densities J^p_i and J^n_i, the hole and electron densities p and n, which are far greater than their perturbations Δp and Δn, respectively.

The associated constitutive equations are obtained as

$$\begin{aligned} \sigma_{ij} &= \frac{\partial U_b}{\partial \varepsilon_{ij}} = c_{ijkl}\varepsilon_{kl} - e_{kij}E_k \\ \sigma_{ijk} &= \frac{\partial U_b}{\partial \eta_{ijk}} = g_{ijklmn}\eta_{lmn} - f_{lijk}E_l \\ D_i &= -\frac{\partial U_b}{\partial E_i} = a_{ij}E_j + e_{ijk}\varepsilon_{jk} + f_{ijkl}\eta_{jkl} \end{aligned} \tag{3}$$

The kinematic equations are expressed as

$$\begin{aligned} &\varepsilon_{ij} = (u_{i,\,j} + u_{j,i})/2 \\ &\eta_{ijk} = \varepsilon_{ij,k} = (u_{i,\,jk} + u_{j,ik})/2 \\ &E_i = -\phi_{,i} \end{aligned} \tag{4}$$

Additionally, the current densities for both electrons and holes are linearized as

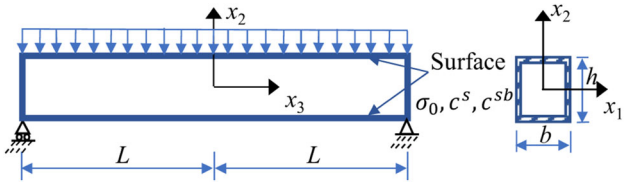

Fig. 1 The schematic diagram of the PSC nanobeam in this work, with the rectangular cross section displayed on the right and the very thin surface layer indicated by the shaded area

$$\begin{aligned} J^p_i &= qp\mu^p_{ij}E_j - qD^p_{ij}p_{,\,j} \cong qp_0\mu^p_{ij}E_j - qD^p_{ij}(\Delta p)_{,\,j} \\ J^n_i &= qn\mu^n_{ij}E_j + qD^n_{ij}n_{,\,j} \cong qn_0\mu^n_{ij}E_j + qD^n_{ij}(\Delta n)_{,\,j} \end{aligned} \tag{5}$$

where initial concentrations of holes and electrons are $p_0 = p - \Delta p$ and $n_0 = n - \Delta n$, respectively. D^p_{ij} and D^n_{ij} denote the diffusion constants of holes and electrons, and μ^p_{ij} and μ^n_{ij} denote the mobilities of holes and electrons, respectively.

Surface elastic constitutive relations based on the GM theory are written as

$$\begin{aligned} &\sigma^s_{\alpha\beta} = \sigma^0_{\alpha\beta} + c^s_{\alpha\beta\gamma\delta}\varepsilon_{\gamma\delta} \\ &\sigma^s_{n\alpha} = \sigma^0_{\alpha\beta}u_{n,\,\beta} \\ &\sigma^s_{i\alpha,\,\alpha} + \sigma^{BS}_{in} = \rho^s\ddot{u}_i \end{aligned} \tag{6}$$

where $\sigma^0_{\alpha\beta}$ denotes surface residual stress components, $c^s_{\alpha\beta\gamma\delta}$ denotes surface elastic constants (surface membrane stiffness), and σ^{BS}_{in} denotes the reaction forces of the bulk core against the surface. On the other hand, surface constitutive equations based on the SO theory are expressed as

$$\begin{aligned} &\sigma^s_{\alpha\beta} = \sigma^0_{\alpha\beta} + c^s_{\alpha\beta\gamma\delta}\varepsilon_{\gamma\delta} \\ &\sigma^s_{n\alpha} = \sigma^0_{\alpha\beta}\mu_{n,\,\beta} \\ &M^s_{\alpha\beta} = c^{sb}_{\alpha\beta\gamma\delta}\kappa_{\gamma\delta} \\ &\sigma^{Ms}_{n\alpha} = M^s_{\alpha\beta,\,\beta} \\ &\sigma^s_{i\alpha,\,\alpha} + \sigma^{BS}_{in} - \sigma^{Ms}_{n\alpha,\,\alpha} = \rho^s\ddot{u}_i \end{aligned} \tag{7}$$

in which $c^{sb}_{\alpha\beta\gamma\delta}$ denotes surface bending stiffness, and $M^s_{\alpha\beta}$ and $\kappa_{\gamma\delta}$ denotes surface bending moment and bending curvature, respectively.

This work considers a simply supported Euler–Bernoulli nanobeam made of n-type ZnO subjected to a uniformly distributed load q_0 (Fig. 1). The length of the nanobeam is $2L$ with a rectangular cross section having a width of b and a height of h. For simplicity, shear deformation is ignored without loss of generality. The hole charge-related terms like Δp are thus omitted in the subsequent calculations. Therefore, the displacement, electric potential, and charge carrier redistribution in the Euler–Bernoulli nanobeam theory are simplified as

Table 1 Material parameters used in this work

Materials	Elastic properties (10^{-12} m^2/N)		Piezoelectric properties (10^{-12} C/N)		Piezoelectric properties (F/m)	
	s_{33}	s_{44}	d_{33}	d_{15}	a_{22}	a_{33}
ZnO	6.94	23.57	11.67	− 11.34	$8.55\varepsilon_0$	$10.2\varepsilon_0$
Si	7.68	12.56	0	0	$11.7\varepsilon_0$	$11.7\varepsilon_0$

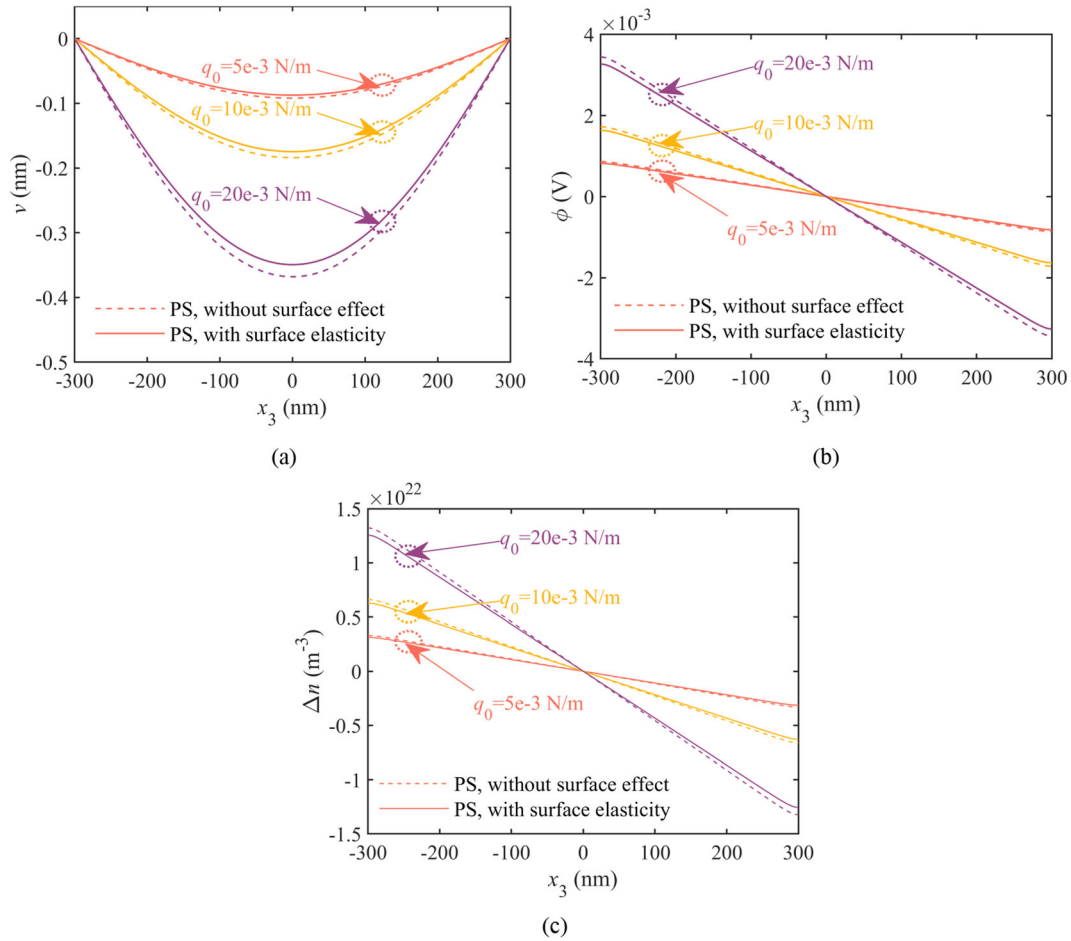

Fig. 2 **a** The deflection, **b** electric potential, and **c** redistribution of charge carriers in the PSC nanobeam when only considering surface membrane stiffness

$$
\begin{aligned}
&u_2(\boldsymbol{x},\, t) \cong v(x_3,\, t)\\
&u_3(\boldsymbol{x},\, t) \cong -x_2 v_{,3}(x_3,\, t)\\
&\phi(\boldsymbol{x},\, \mathrm{t}) \cong x_2 \phi^{(1)}(x_3,\, t)\\
&\Delta n(\boldsymbol{x},\, \mathrm{t}) \cong x_2 n^{(1)}(x_3,\, t)
\end{aligned}
\tag{8}
$$

in which the superscript $^{(1)}$ indicates they are the first-order components of ϕ and n after they are expanded into power series. By ignoring the higher-order elstic terms, the stresses, electric displacements, and current densities are thus

$$
\begin{aligned}
&\sigma_{33} = \bar{c}_{3333}\varepsilon_{33} - \bar{e}_{333}E_3\\
&\sigma_{332} = -f_{2332}E_2\\
&D_2 = \bar{a}_{22}E_2 + f_{2332}\eta_{332}\\
&D_3 = \bar{a}_{33}E_3 + \bar{e}_{333}\varepsilon_{33}\\
&J_2^n = qn_0\mu_{22}^n E_2 + qD_{22}^n(\Delta n)_{,2}\\
&J_3^n = qn_0\mu_{33}^n E_3 + qD_{33}^n(\Delta n)_{,3}
\end{aligned}
\tag{9}
$$

Surface stresses are thus written as

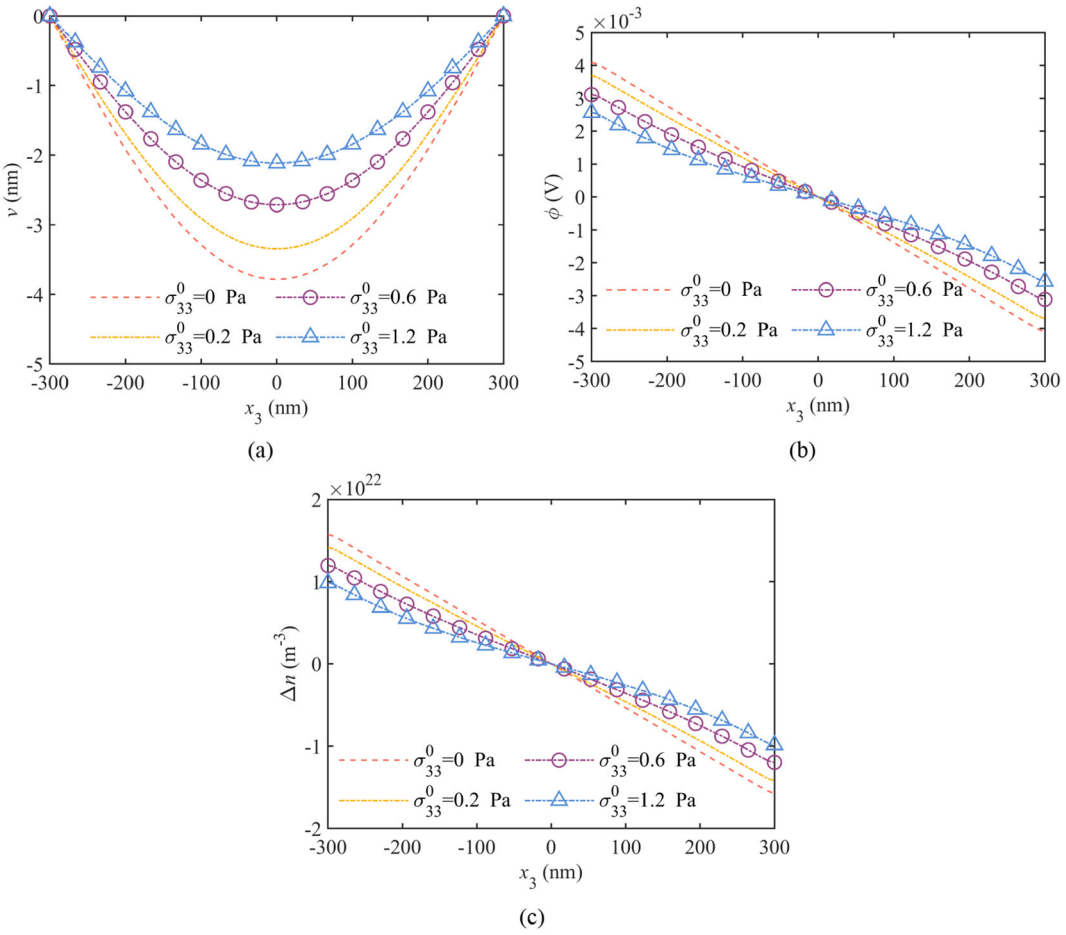

Fig. 3 Surface residual stress effect on **a** the deflection, **b** electric potential, and **c** redistribution of charge carriers in the PSC nanobeam

$$
\begin{aligned}
&\kappa_{33} = u_{2,33} = v_{,33}\\
&\sigma^s_{33} = \sigma^0_{33} + c^s_{33}\varepsilon_{33}\\
&\sigma^s_{23} = \sigma^0_{33}\mu_{2,3} = \sigma^0_{33}v_{,3}\\
&M^s_{33} = c^{sb}_{33}\kappa_{33} = c^{sb}_{33}v_{,33}\\
&\sigma^{Ms}_{23} = M^s_{33,3} = c^{sb}_{33}v_{,333}
\end{aligned}
\tag{10}
$$

in which $c^s_{33} = c^s_{3333}$ and $c^{sb}_{33} = c^{sb}_{3333}$.

The reaction force of interior body to the surface stress is

$$
\begin{aligned}
&\sigma^{BS}_{32} = -\sigma^s_{33,3} + \rho^s\ddot{u}_3\\
&\sigma^{BS}_{22} = -\sigma^s_{23,3} + \sigma^{Ms}_{23,3} + \rho^s\ddot{u}_2
\end{aligned}
\tag{11}
$$

Finally, the 1D equilibrium equations for the Euler–Bernoulli nanobeam are obtained as

$$
\begin{aligned}
&-(\bar{c}_{3333}I + c^s_{33}I^s + 2bc^{sb}_{33})v_{,3333} + 2b\sigma^0_{33}v_{,33} + \bar{e}_{333}I\phi^{(1)}_{,333} + f_{2332}A\phi^{(1)}_{,33} = q_0\\
&-\bar{e}_{333}Iv_{,333} + f_{2332}Av_{,33} - \bar{a}_{33}I\phi^{(1)}_{,33} + \bar{a}_{22}A\phi^{(1)} = -qIn^{(1)}\\
&-qn_0\mu^n_{33}I\phi^{(1)}_{,33} + qn_0\mu^n_{22}A\phi^{(1)} + qD^n_{33}I\phi^{(1)}_{,33} - qD^n_{22}A\phi^{(1)} = 0
\end{aligned}
\tag{12}
$$

The boundary conditions for a simply supported nanobeam are set as

$$
\begin{aligned}
&v(-L) = v(L) = 0\\
&M(-L) = M(L) = 0\\
&D^{(1)}_3(-L) = D^{(1)}_3(L) = 0\\
&J^{n(1)}_3(-L) = J^{n(1)}_3(L) = 0
\end{aligned}
\tag{13}
$$

where the bending moment M, electric displacement D_i, and current density J_i at the boundaries are expressed as

$$
\begin{aligned}
&M = \bar{c}_{3333}Iv_{,33} + \bar{e}_{333}I\phi^{(1)}_{,3} + f_{2332}A\phi^{(1)}\\
&D^{(1)}_3 = -\bar{a}_{33}I\phi^{(1)}_{,3} - \bar{e}_{333}Iv_{,33}\\
&J^{n(1)}_3 = -qn_0\mu^n_{33}I\phi^{(1)}_{,3} + qD^n_{33}In^{(1)}_{,3}
\end{aligned}
\tag{14}
$$

The general solution is postulated as

$$
\begin{aligned}
&v = C_1e^{\lambda x_3}\\
&\phi^{(1)} = C_2e^{\lambda x_3}\\
&n^{(1)} = C_3e^{\lambda x_3}
\end{aligned}
\tag{15}
$$

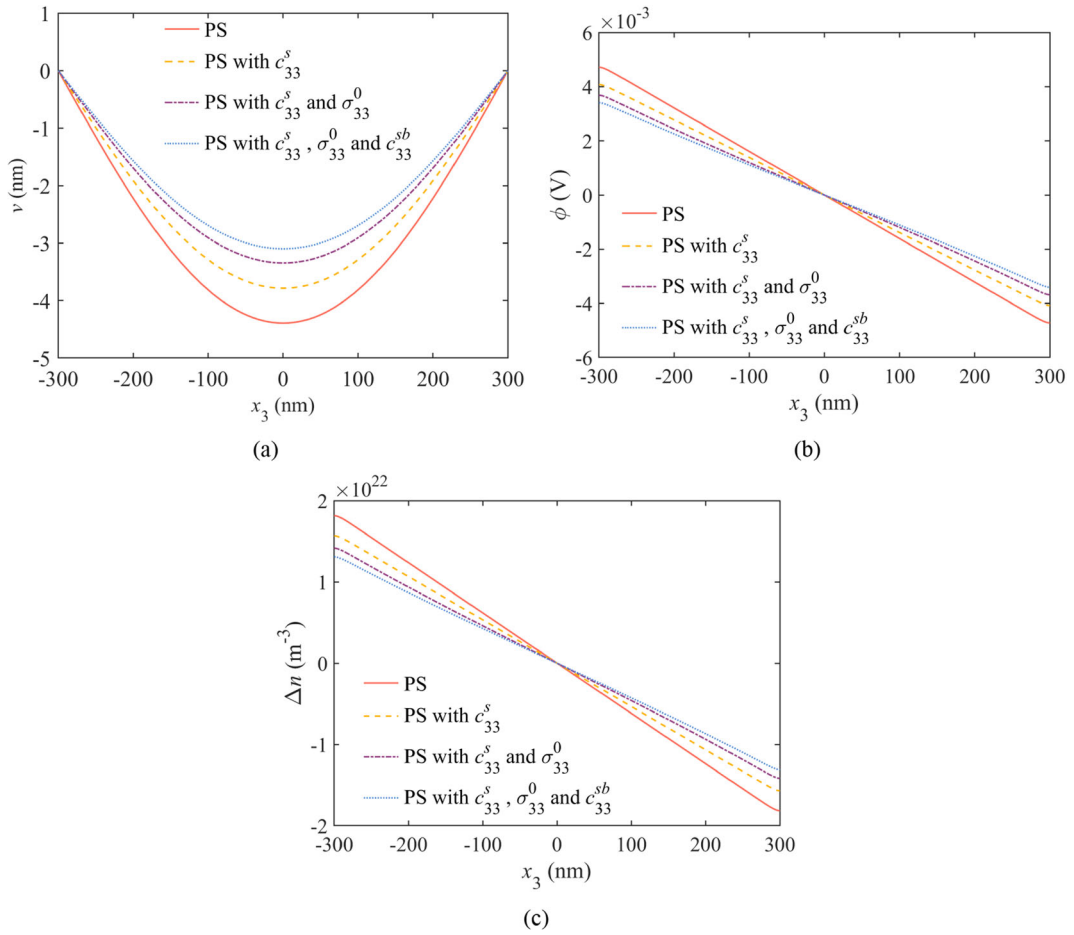

Fig. 4 Complete surface elastic effects on **a** the deflection, **b** electric potential, and **c** redistribution of charge carriers in the PSC nanobeam

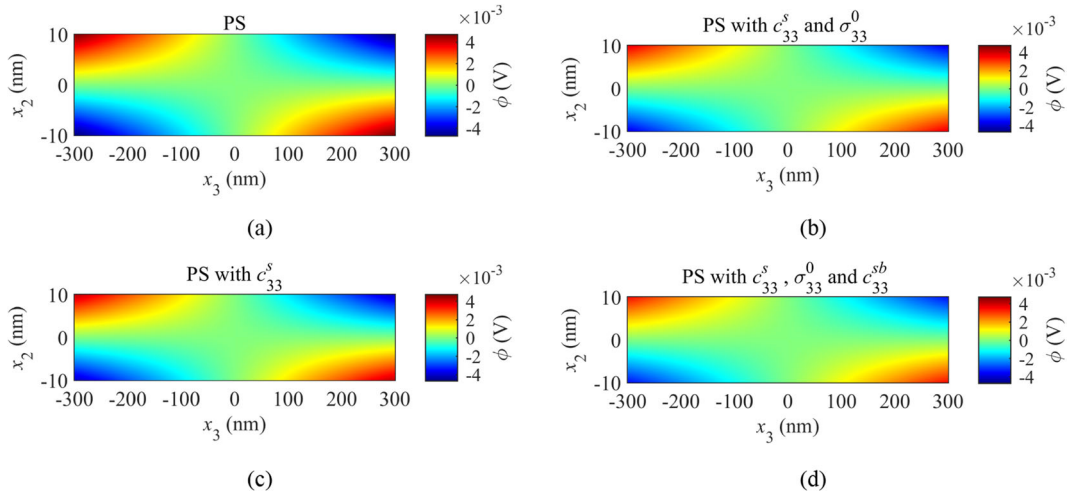

Fig. 5 Electric potential distribution in the PSC nanobeam considering **a** piezoelectric effect only, **b** piezoelectric effect as well as surface residual stress and surface membrane stiffness, **c** piezoelectric effect and surface membrane stiffness, and **d** piezoelectric effect with complete surface elastic effects across the longitudinal section

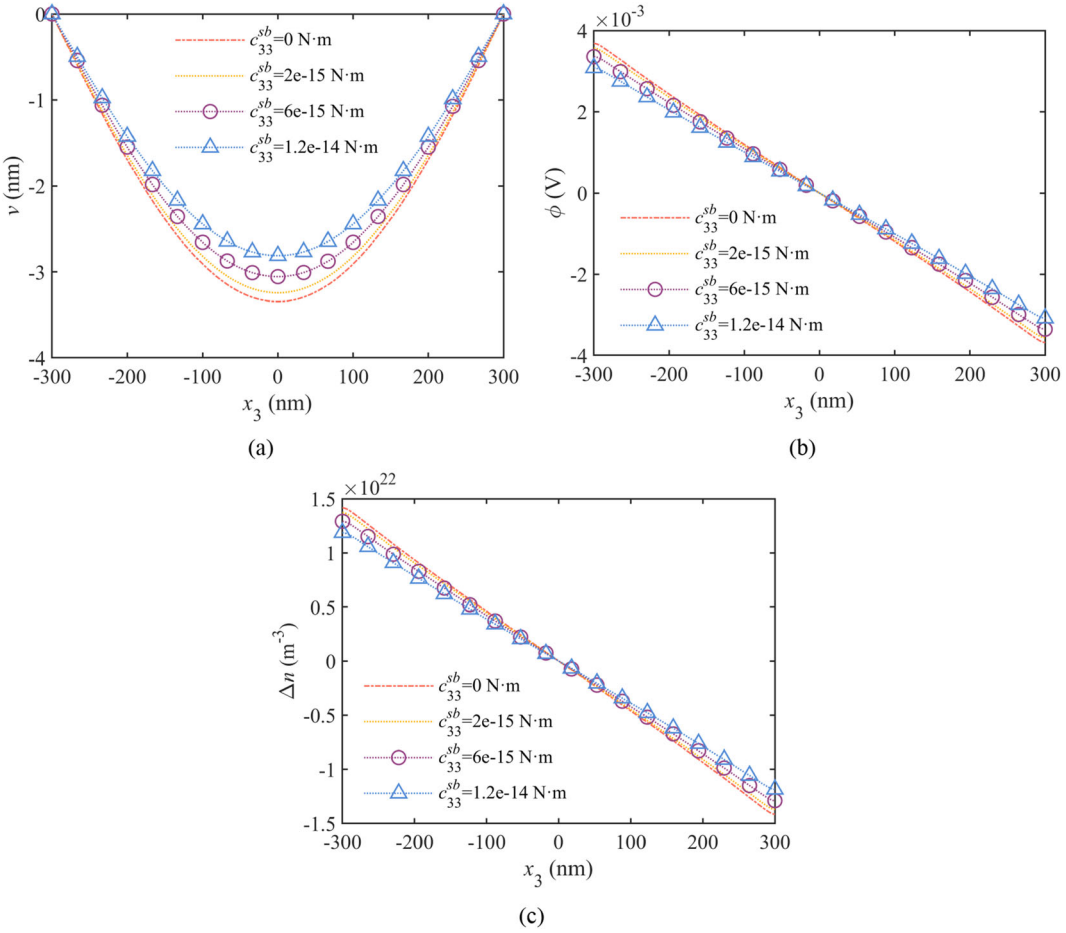

Fig. 6 The surface flexural rigidity effect on the PSC nanobeam without considering flexoelectricity

The particular solution can be set as

$$v = C_1^{l+1} x_3^{l-a},\ \phi^{(1)} = C_2^{l+1} x_3^{l-a} \tag{16}$$

As a result, the final solution takes the following form,

$$\begin{aligned} v &= \sum_{m=1}^{a} C_1^m \mathrm{e}^{\lambda m x_3} + \sum_{m=a+1}^{l} C_1^m x_3^{m-a-1} + C_1^{l+1} x_3^{l-a} \\ \phi^{(1)} &= \sum_{m=1}^{a} C_2^m \mathrm{e}^{\lambda m x_3} + \sum_{m=a+1}^{l} C_2^m x_3^{m-a-1} + C_2^{l+1} x_3^{l-a} \\ n^{(1)} &= \frac{C_3}{C_2}\phi^{(1)} = \frac{n_0 \mu_{33}^n}{D_{33}^n}\phi^{(1)} = \frac{n_0 \mu_{22}^n}{D_{22}^n}\phi^{(1)} \end{aligned} \tag{17}$$

where $\mu_{33}^n / D_{33}^n = \mu_{22}^n / D_{22}^n = q/k_B T$, k_B is the Boltzmann constant, and T is set as 300 K.

3 Results and Discussion

Table 1 summarizes the elastic and electromechanical material parameters used in this study, unless otherwise specified. Due to difficulties in experimental measurement of surface elastic constants, the surface membrane stiffness is determined based on a proportional relationship $\boldsymbol{c}^s = h_0 \boldsymbol{c}$, and the intrinsic material length h_0 is fixed as 0.4 nm in this work [45]. The surface residual stress is set similar to other literature, except for parametric studies. For similar argument, the flexoelectric constants are also given according to [5]. It is worthwhile to emphasize that although these material coefficients may be challenging to obtain at present, parametric studies still provide valuable insights for the underling mechanism. ε_0 is the dielectric constant of vacuum 8.5×10^{-12} F/m. The carrier mobility is set as $\mu_{22}^n = \mu_{33}^n = 1\ \mathrm{m}^2/\mathrm{Vs}$, and the diffusion constants $D_{22}^n = D_{33}^n = 0.026\ \mathrm{m}^2/\mathrm{s}$.

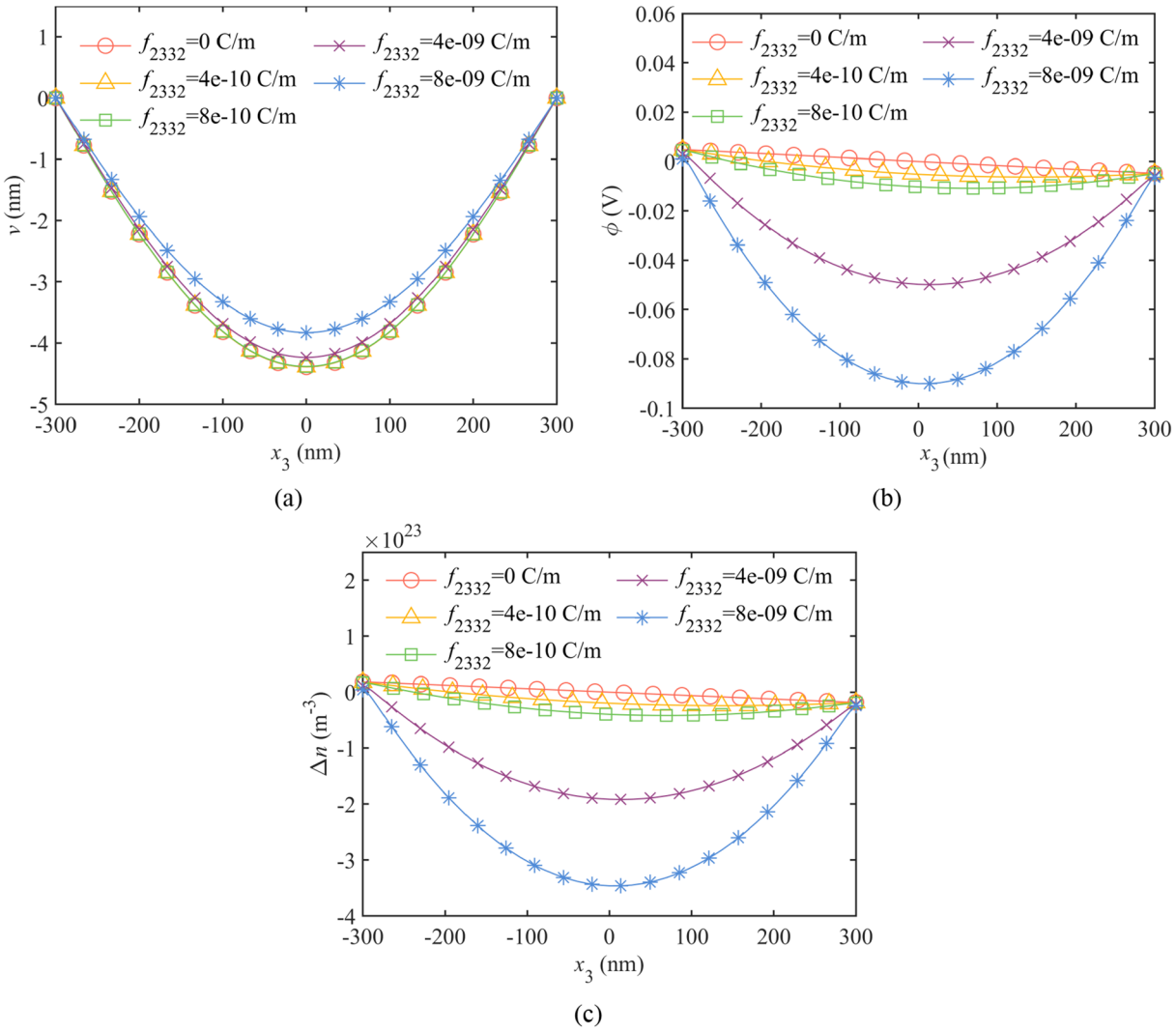

Fig. 7 Flexoelectric effect on **a** the deflection, **b** electric potential, and **c** redistribution of charge carriers in the PSC nanobeam

3.1 Piezoelectricity and Surface Elasticity

First and foremost, our numerical results, without involving any surface effect, align well with earlier findings reported by Zhang et al. [45] However, upon considering surface elastic effects (See Fig. 2), we notice that our results only agree accurately with theirs for relatively small loads; larger forces lead to significant discrepancies. This can be attributed to the absence of surface piezoelectric properties in our work. As a result, to isolate the impact of the surface piezoelectric effect, q_0 is set to be of a relatively small value of 5×10^{-3} N/m in the subsequent discussions for comparison purposes. The largest deflection occurs at the midpoint of the nanobeam, where the electric potential and redistribution of charge carriers are nullified due to the problem's symmetric nature. The deflection increases as a larger force is applied, and the electric potential and the redistribution of charge carriers decrease linearly along the length. Additionally, the maximum/minimum electric potential is observed at both ends of the nanobeam. To clarify the significance of surface residual stress effect, the dependence of deflection, electric potential, and redistribution of charge carriers on it is calculated. Consistent with other reports [45], the nanobeam becomes stiffer with increasing surface residual stress (Fig. 3), resulting in reduced deflections. It is important to note that in this analysis, only positive residual stresses are considered, and negative ones may yield opposite observations. Similarly, the electric potential and thus redistribution of charge carriers decrease with rising surface residual stresses.

In the subsequent numerical examples, surface residual stress, surface membrane stiffness, and surface flexural rigidity are altogether considered. Compared to the intrinsic PSC

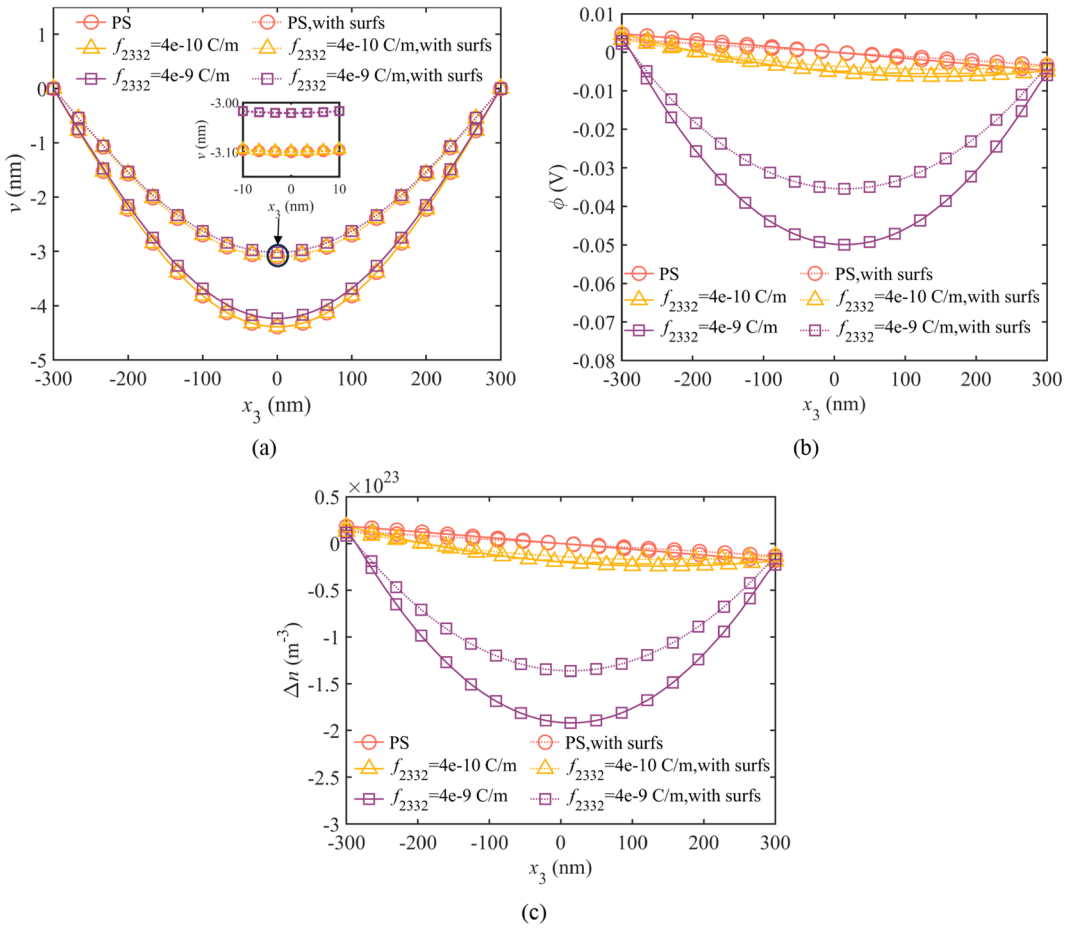

Fig. 8 Flexoelectric effect together with complete surface elastic effects on **a** the deflection, **b** electric potential, and **c** redistribution of charge carriers of the PSC nanobeam. For comparison purpose, the piezoelectric effect together with complete surface elastic effects is also presented

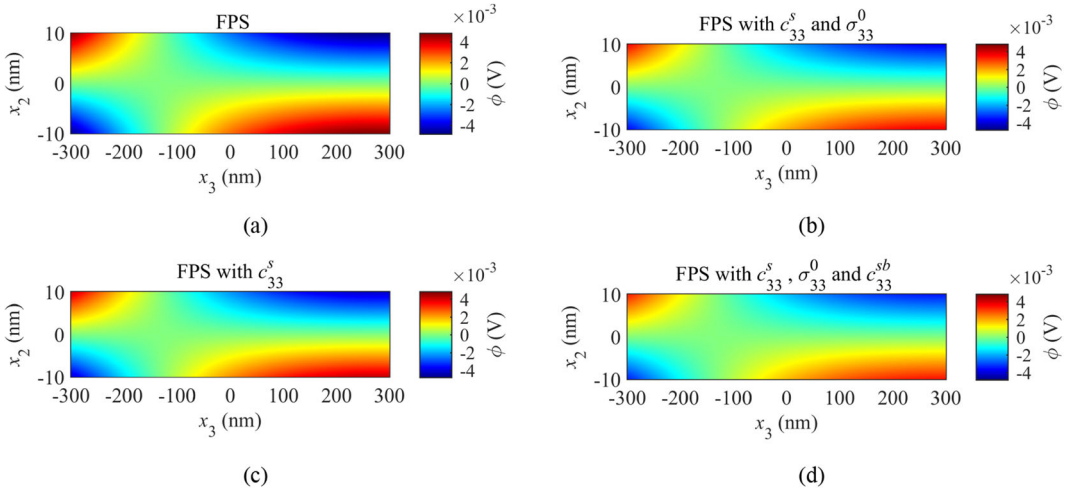

Fig. 9 Electric potential in the PSC nanobeam considering **a** piezo-flexoelectric effect only, **b** piezo-flexoelectric and residual and surface elastic effects, **c** piezo-flexoelectric and surface elastic effects, and **d** piezo-flexoelectric and complete surface elastic effects across the cross section

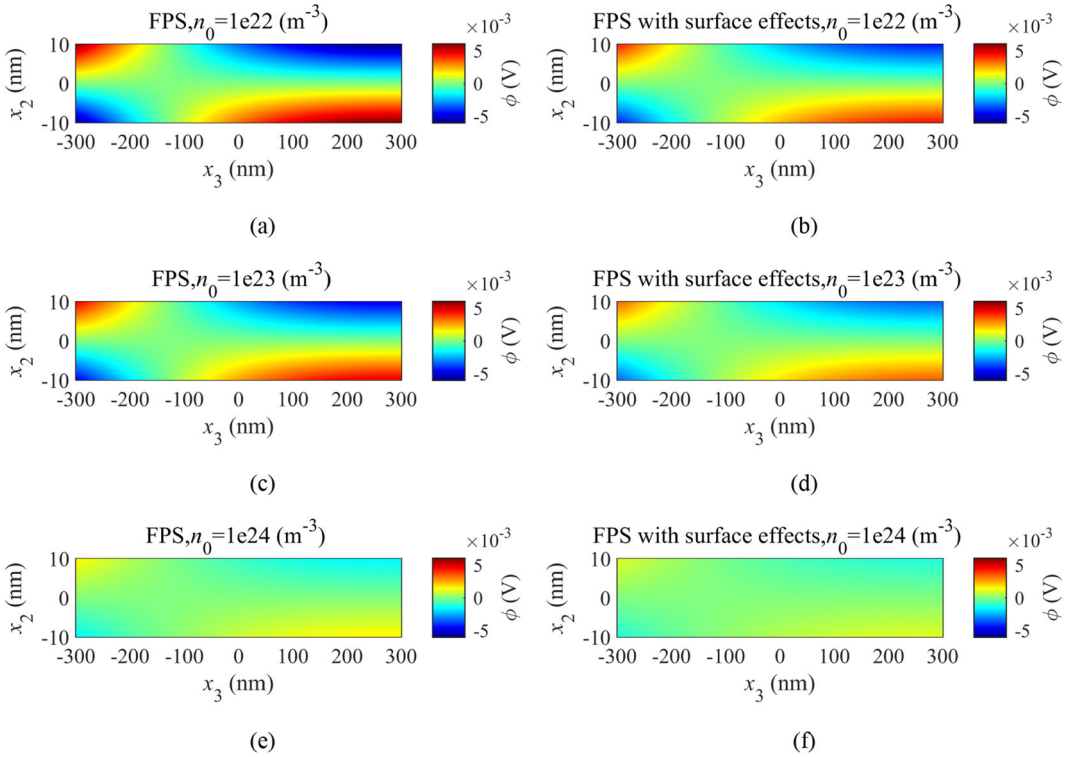

Fig. 10 Electric potential in the PSC nanobeam with different initial carrier concentrations: **a** FPS with n_0 being 10^{22}, **c** FPS with n_0 being 10^{23}, and **e** FPS with n_0 being 10^{24} without considering surface effects; and **b** FPS with n_0 being 10^{22}, **d** FPS with n_0 being 10^{23}, and **f** FPS with n_0 being 10^{24} considering complete surface elastic effects across the longitudinal section

nanobeam, the deflection is reduced as any surface elastic effect incorporated. In particular, the introduction of complete surface elastic properties, including surface membrane stiffness and flexural rigidity, can further reduce the deflection by about 2/3, essentially stiffening the nanobeam (Fig. 4a). This result is consistent with the findings of the pure elastic problem on a nanobeam [32]. Both electric potential and redistribution of charge carriers exhibit a similar decreasing trend, as shown in Fig. 4b and c. Notably, the surface bending stiffness does show a pronounced effect on electromechanical behavior and the motion of charge carriers, as illustrated in Fig. 4. This effect seems to have been overlooked in the previous literature. In Fig. 5, one can further observe the effects of complete surface elastic properties on the distribution of the electric potential. The electric potential primarily changes at four corners of the nanobeam. Additionally, it is noted that the surface bending stiffness has a smaller effect compared to surface residual stress and membrane stiffness on the electric potential.

To further investigate the influence of surface bending stiffness, the surface flexural rigidity is varied from zero to a relatively great value. Similar to the effect of surface residual stress, the PSC beam stiffens as surface flexural rigidity increases (Fig. 6). In particular, it appears that surface bending stiffness can be disregarded when its magnitude is less than 10^{-15}. The electric potential and redistribution of charge carriers also decrease as surface bending stiffness increases.

3.2 Flexoelectricity Without Surface Effect

In this section, the flexoelectric effect is studied in the PSC nanobeam without considering any surface effect, by varying the flexoelectric coefficient from zero to a relatively high value. It is evident that the increasing flexoelectric effect indeed enhances the effective bending stiffness, as indicated by decreased deflection as shown in Fig. 7a. Compared to the linear distributions of electric potential and charge carriers in the presence of only piezoelectricity, their distributions become nonlinear and asymmetric due to the superposition of the piezoelectric and flexoelectric effects. We observe that the stronger is the flexoelectric effect, the larger the electric potential and redistribution of charge carriers at the midpoint of the PSC beam can be achieved, as shown in Fig. 7b and c. More importantly, it is noticed that the difference in electric quantities at the two ends of the beam remains nearly unchanged for increased flexoelectric effect.

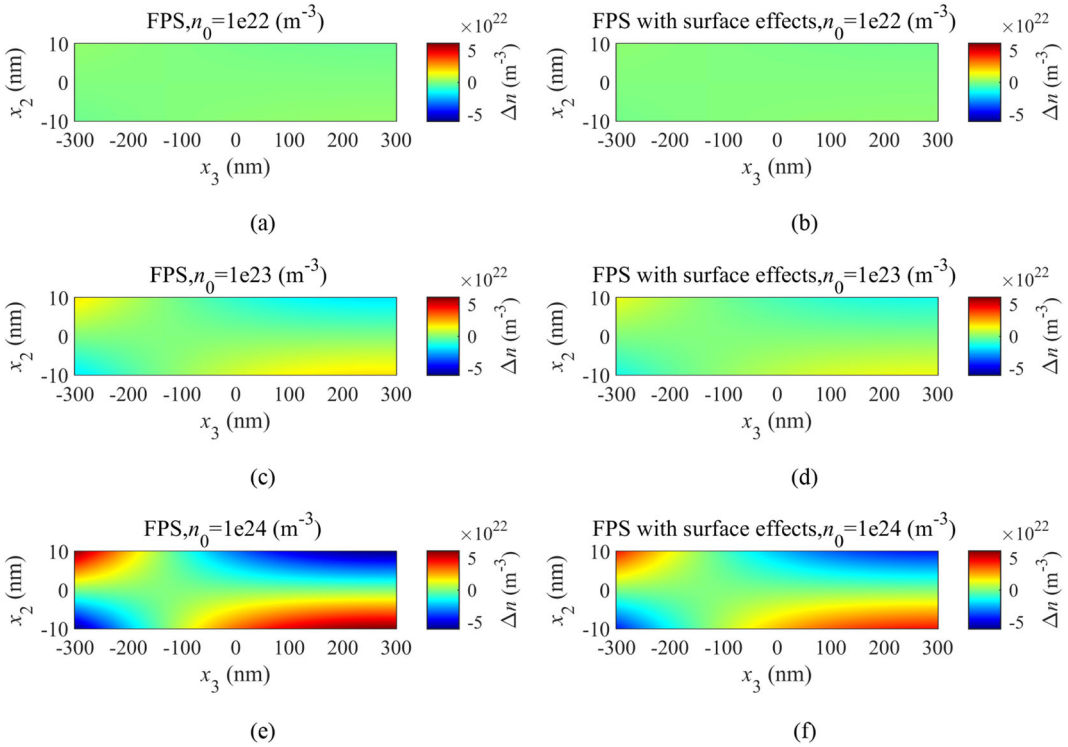

Fig. 11 Distribution of carriers in the PSC nanobeam with different initial carrier concentrations: **a** FPS with n_0 being 10^{22}, **c** FPS with n_0 being 10^{23}, and **e** FPS with n_0 being 10^{24} without considering surface effects; and **b** FPS with n_0 being 10^{22}, **d** FPS with n_0 being 10^{23}, and **f** FPS with n_0 being 10^{24} considering complete surface elastic effects across the longitudinal section

3.3 Flexoelectricity with Surface Effect

Now, both the complete surface elastic effects and flexoelectric effect are considered in the PSC nanobeam. From Fig. 8, it is clearly seen that surface elasticity has a greater impact on deflection when comparing the solid and dashed lines. In contrast, flexoelectricity demonstrates a more prominent effect on the electric quantities (as indicated by the markers in the figure). Both surface elastic and flexoelectric effects enhance the effective bending stiffness. Moreover, the incorporation of complete surface elastic effects results in a reduction in maximum deflection and electric quantities in the PSC nanobeam. It should be pointed out that such enhancement depends on the sign of surface elastic constants, as discussed in [43], where it is also stated that the negative values weaken the bending stiffness of the nanobeam. In particular, through careful numerical studies, it is noticed that the flexoelectricity begins to affect electromechanical responses when its magnitude reaches approximately 10^{-9} C/m. Their effects on the electric potential distribution across the cross section of the nanobeam can be further observed in Fig. 9. It is noticed that the electric potential distributes across a larger area and achieves greater extreme values in the nanobeam without surface effect compared to the one in the presence of the surface. Furthermore, a comparison between Figs. 5a and 9a reveals that the electric distribution across the rectangular cross section becomes asymmetric and covers a larger area.

The motion of charge carriers also plays a vital role in the performance of semiconductors. As the initial doping density of charge carriers increases, the electric potentials and their distribution decrease because of the screening effect (Figs. 10a, c, and e, and b, d, and f) regardless of whether surface elastic effects are considered or not. This validates that surface elastic properties have a minimal impact on electric potential distribution. Similarly, charge carrier redistribution can also be tuned through the initial doping concentration. It can be observed from Figs. 11a–f that redistribution is insignificant for lower initial concentrations, but becomes more pronounced for higher initial concentrations. Moreover, the initial doping density of charge carriers has a negligible effect on the deflection.

The surface elastic and flexoelectric effects on intrinsic semiconductors are also of interest. For instance, similar calculations are conducted on a nanobeam made of silicon. As shown in Fig. 12a, the introduction of surface elastic effects results in an increase in the effective bending rigidity of the beam. In contrast, surface elastic effects reduce the electric quantities, particularly when the flexoelectric coefficient is larger (Figs. 12b and c). This observation may become clearer in the electric potential distribution along the height of the

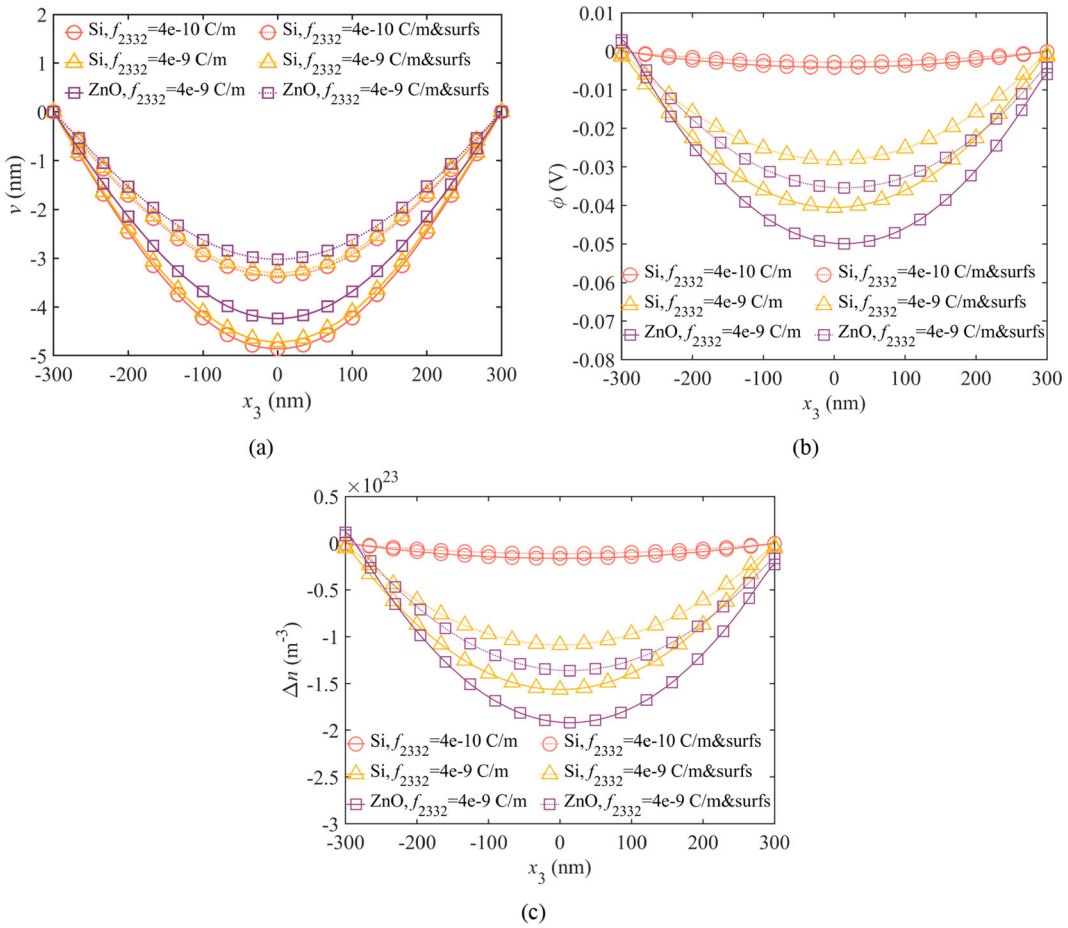

Fig. 12 Flexoelectric effect together with complete surface elastic effects on **a** the deflection, **b** electric potential, and **c** redistribution of charge carriers in a silicon nanobeam. For comparison purpose, the results for a ZnO nanobeam are also presented

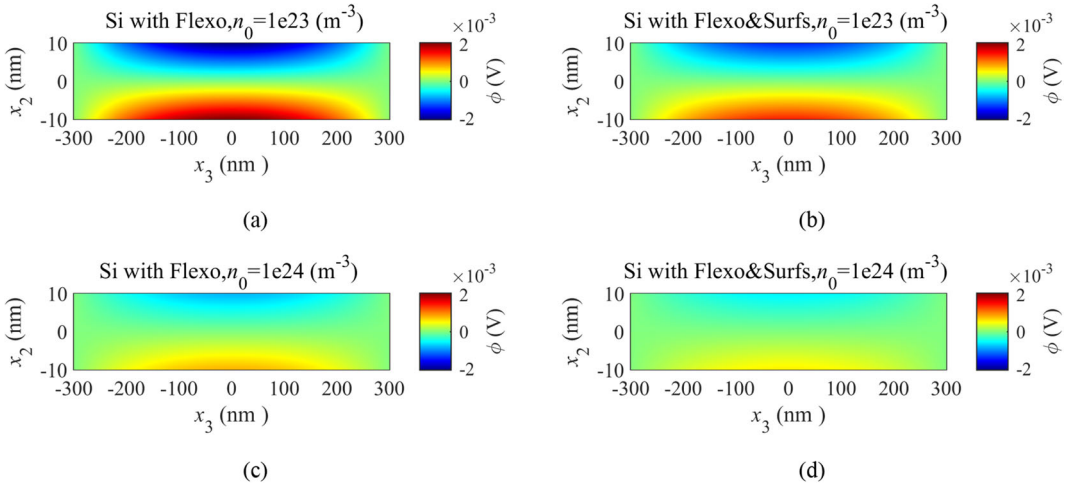

Fig. 13 Electric potential along the longitudinal section in the silicon nanobeam including **a** flexoelectricity only, **b** flexoelectricity and complete surface elastic effects, with an initial charge carrier density of 10^{23} m^{-3}, **c** flexoelectricity only, and **d** flexoelectricity and complete surface elastic effects, with an initial charge carrier density of 10^{24} m^{-3}

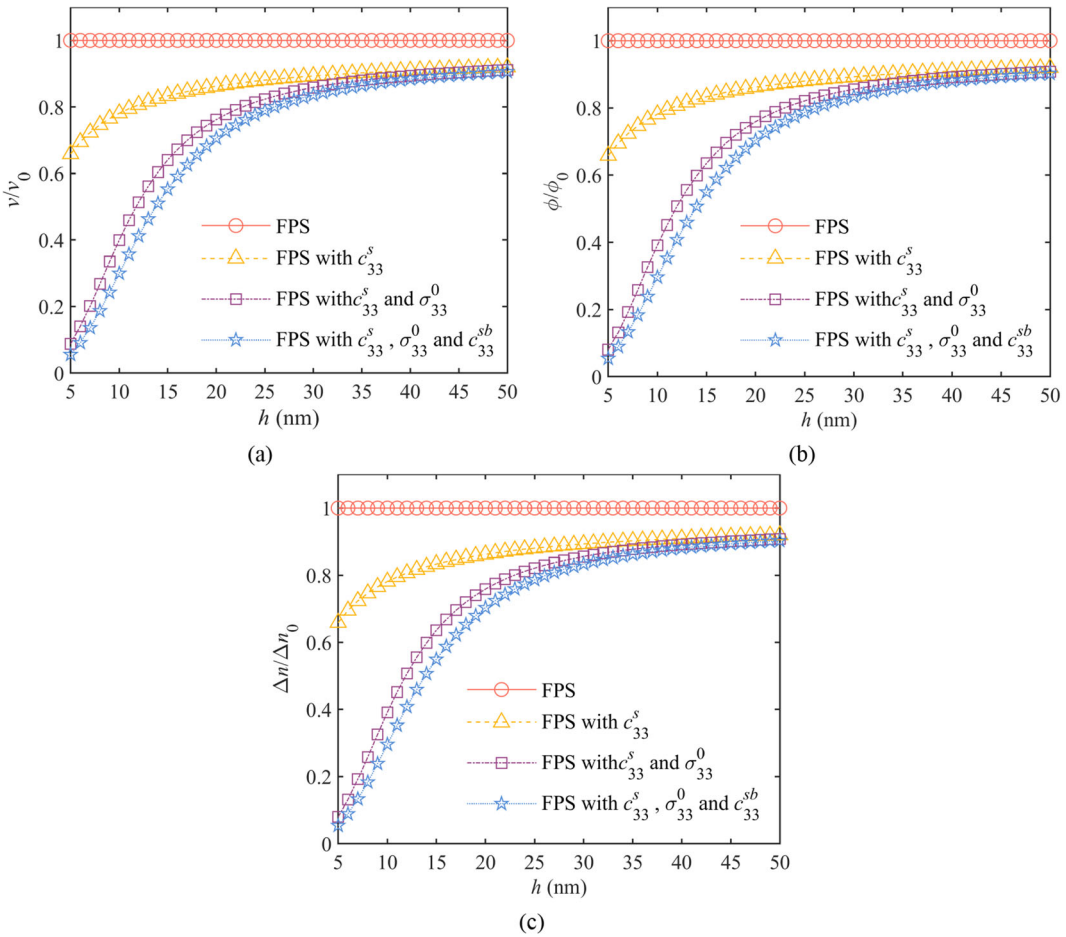

Fig. 14 Size effect on **a** the deflection, **b** electric potential, and **c** redistribution of charge carriers in the PSC nanobeam considering flexoelectric effect. The deflection and electric quantities are normalized by the values obtained in the absence of any surface elastic effect

silicon nanobeam, as shown in Figs. 13a and b. Moreover, the screening effect of charge carriers can also be seen in Figs. 13a and c, in which the initial density of charge carriers is higher. One may also notice that the flexoelectric effect in silicon is weaker than that in PSCs, although identical coefficients are assumed. Nevertheless, the flexoelectric effect remains an effective way to tune electronic behaviors, particularly in the absence of piezoelectricity. From Fig. 13, it is also observed that the electric potential symmetrically distributes along the length and vanishes at the two ends of the beam, which differs from ZnO nanobeam behavior due to the existence of piezoelectric effect, as shown in Figs. 5 and 9.

3.4 Size Effect

Last but not least, it is known that the flexoelectric effect is induced by the strain gradient, which typically becomes more significant as the structural size decreases to nanoscale. In fact, both surface elasticity and flexoelectricity show size-dependent characteristics. Therefore, it is also of great interest to explore the size effect on electromechanical coupling behaviors in a PSC nanobeam when considering flexoelectricity. As shown in Fig. 14, the height exhibits a clear size effect on both deflection and electric quantities, repented by values at the midpoint of the PSC nanobeam, especially for those with a height $h \leq \sim 30$ nm when considering surface elastic effects. It is evident that among all surface elastic moduli, surface membrane stiffness and surface residual stress show more prominent effect than surface bending stiffness at small sizes, while such differences diminish as sizes increase.

4 Conclusions

In summary, the governing equations and associated constitutive relations for a piezoelectric semiconducting nanobeam were established, considering full surface elastic effects such as surface residual stress, surface membrane, and surface bending stiffness, as well as the flexoelectric effect. It was found that surface elastic properties have a significant impact on the deflection of a PSC nanobeam, while the flexoelectric

effect plays a more dominant role in electric quantities such as electric potential and the redistribution of charge carriers. In particular, both surface elastic and flexoelectric effects may enhance the bending rigidity and reduce the deflection depending on their signs and magnitude. The presence of the flexoelectric effect disrupts the antisymmetric linear distribution of these electric quantities. Additionally, the initial carrier doping density plays a crucial role in electromechanical behaviors. Moreover, it is evident that both surface elastic and flexoelectric effects vary with size. The results of this work can provide valuable insights for the design of nanoscale electronic devices based on PSCs.

Acknowledgements We wish to acknowledge the support of the National Natural Science Foundation of China [Grant number: 11702076], and the Natural Science Foundation of Anhui Province [Grant numbers: 2208085MA17 and 2208085ME129].

Declarations

Conflict of interest The authors declare that they have no known competing financial interests or personal relationships that could have appeared to influence the work reported in this paper.

References

1. Wang ZL. Progress in piezotronics and piezo-photonics. Adv Mater. 2012;24:4632–46.
2. Yang JS. Analysis of piezotronics semiconductor structures. Berlin: Springer Nature Switzerland AG; 2020.
3. Song JH, Zhou J, Wang ZL. Piezoelectric and semiconducting coupled power generating process of a single ZnO belt/wire: a technology for harvesting electricity from the environment. Nano Lett. 2006;6(8):1656–62.
4. Kumar B, Kim SW. Energy harvesting based on semiconducting piezoelectric ZnO nanostructures. Nano Energy. 2012;1:342–55.
5. Auld BA. Acoustic fields and waves in solids, vol. 1. New York: Wiley; 1973.
6. Yang WL, Hu YT, Yang JS. Transient extensional vibration in a ZnO piezoelectric semiconductor nanofiber under a suddenly applied end force. Mater Res Express. 2019;6:025902.
7. Yang JS, Zhou HG. Amplification of acoustic waves in piezoelectric semiconductor plates. Int J Solids Struct. 2005;42:3171–83.
8. Wang ZL. Piezotronics and piezo-phototronics. Berlin: Springer; 2012.
9. Zhou XF, Shen B, Lyubartsev A, Zhai JW, Hedin N. Semiconducting piezoelectric heterostructures for piezo- and piezophotocatalysis. Nano Energy. 2022;96:107141.
10. Guo YF, Wang ZL. Equilibrium potential of free charge carriers in a bent piezoelectric semiconductive nanowire. Nano Lett. 2009;9:1103–10.
11. Zhang CL, Wang XY, Chen WQ, Yang JS. An analysis of the extension of a ZnO piezoelectric semiconductor nanofiber under an anial force. Smart Mater Struct. 2017;26:025030.
12. Fan SQ, Liang YX, Xie JM, Hu YT. Exact solutions to the electromechanical quantities inside a statically-bent circular zno nanowire by taking into account both the piezoelectric property and the semiconducting performance: part I– linearized analysis. Nano Energy. 2017;40:82–7.
13. Cheng RR, Zhang CL, Chen WQ, Yang JS. Piezotronic effects in the extension of a composite fiber of piezoelectric dielectrics and nonpiezoelectric semiconductors. J Appl Phys. 2018;124:064506.
14. Ma LL, Chen WJ, Zheng Y. Flexoelectric effect at the nanoscale. In: Schmauder S, Chen CS, Chawla K, Chawla N, Chen W, Kagawa Y, editors. Handbook of mechanics of materials. Singapore: Springer; 2018. p. 1–42.
15. Liu C, Wu HP, Wang J. Giant piezoelectric response in piezoelectric/dielectric superlattices due to flexoelectric effect. Appl Phys Lett. 2016;109:192901.
16. Majdoub MS, Sharma P, Cagin T. Enhanced size-dependent piezoelectricity and elasticity in nanostructures due to the flexoelectric effect. Phys Rev B. 2008;77:125424.
17. Zhou ZD, Yang CP, Su YX, Huang R, Lin XL. Electromechanical coupling in piezoelectric nanobeams due to the flexoelectric effect. Smart Mater Struct. 2017;26:095025.
18. Qu YL, Jin F, Yang JS. Effects of mechanical fields on mobile charges in a composite beam of flexoelectric dielectrics and semiconductors. J Appl Phys. 2020;127:194502.
19. Wang KF, Wang BL. Electrostatic potential in a bent piezoelectric nanowire with consideration of size-dependent piezoelectricity and semiconducting characterization. Nanotechnology. 2018;29:255405.
20. Zhao MH, Liu X, Fan CY, Lu CS, Wang BB. Theoretical analysis on the extension of a piezoelectric semi-conductor nanowire: effects of flexoelectricity and strain gradient. J Appl Phys. 2020;127: 085707.
21. Zhao MH, Niu JN, Lu CS, Wang BB, Fan CY. Effects of flexoelectricity and strain gradient on bending vibration characteristics of piezoelectric semiconductor nanowires. J Appl Phys. 2021;129:164301.
22. Sun L, Zhang ZC, Gao CF, Zhang CL. Effect of flexoelectricity on piezotronic responses of a piezoelectric semiconductor bilayer. J Appl Phys. 2021;129:244102.
23. Qu YL, Jin F, Yang JS. Bending of a flexoelectric semiconductor plate. Acta Mech Solida Sin. 2022;35(3):434–45.
24. Guo JY, Nie GQ, Liu JX, Zhang LL. Free vibration of a piezoelectric semiconductor plate. Eur J Mech/A Solids.2022;95:104647.
25. Gurtin ME, Murdoch AI. A continuum theory of elastic material surfaces. Arch Ration Mech Anal. 1975;57:291–323.
26. Gurtin ME, Murdoch AI. Surface stress in solids. Int J Solids Struct. 1978;14:431–40.
27. Duan HL, Wang J, Karihaloo BL, Huang ZP. Nanoporous materials can be made stiffer than non-porous counterparts by surface modification. Acta Mater. 2006;54(11):2983–90.
28. Ansari R, Sahmani S. Surface stress effects on the free vibration behavior of nanoplates. Int J Eng Sci. 2011;49(11):1204–15.
29. Yan Z, Jiang LY. Vibration and buckling analysis of a piezoelectric nanoplate considering surface effects and in-planie constraint. Proc Royal Soc A. 2012;468:3458–75.
30. Huang DW. Size-dependent response of ultra-thin films with surface effects. Int J Solids Struct. 2008;45:568–79.
31. Steigmann DJ, Ogden RW. Plane deformations of elastic solids with intrinsic boundary elasticity. Proc Royal Soc London A Math Phys Eng Sci. 1959;453:853–77.
32. Chhapadia P, Mohammadi P, Sharma P. Curvature-dependent surface energy and implications for nanostructures. J Mech Phys Solids. 2011;59:2103–15.
33. Mohammadi P, Sharma P. Atomistic elucidation of the effect of surface roughness on curvature-dependent surface energy, surface stress, and elasticity. Appl Phys Lett. 2012;100:133110–4.
34. Neffati D, Kulkarni Y. Homogenization of surface energy and elasticity for highly rough surfaces. J Appl Mech. 2022;89:041004.
35. Ban YX, Mi CW. Analytical solutions of a spherical nanoinhomogeneity under far-field unidirectional loading based on Steigmann-Ogden surface model. Math Mech Solids. 2020;25:1904–23.

36. Li XB, Mi CW. Effects of surface tension and steigmann-ogden surface elasticity on hertzian contact properties. Int J Eng Sci. 2019;145:103165.
37. Shen SP, Hu SL. A theory of flexoelectricity with surface effect for elastic dielectrics. J Mech Phys Solids. 2010;58:665–77.
38. Liang X, Hu SL, Shen SP. Effects of surface and flexoelectricity on a piezoelectric nanobeam. Smart Mater Struct. 2014;23:035020.
39. Xu XJ, Deng ZC, Wang B. Closed solutions for the electromechanical bending and vibration of thick piezoelectric nanobeams with surface effects. J Phys D Appl Phys. 2013;46:405302–11.
40. Wang KF, Wang BL. Effects of surface and interface energies on the bending behavior of nanoscale multilayered beams. Physica E. 2013;54:197–201.
41. Zhu CS, Fang XQ, Liu JX, Li HY. Surface energy effect on nonlinear free vibration behavior of orthotropic piezoelectric cylindrical nano-shells. Eur J Mech A/Solids. 2017;66:423–32.
42. Yan Z, Jiang LY. Size-dependent bending and vibration behavior of piezoelectric nanobeams due to flexoelectricity. J Phys D Appl Phys. 2013;46:355502.
43. Shingare KB, Kundalwal SI. Flexoelectric and surface effects on the electromechanical behavior of graphene-based nanobeams. Appl Math Model. 2020;81:70–91.
44. Mizzi CA, Marks LD. The role of surfaces in flexoelectricity. J Appl Phys. 2021;129:224102.
45. Zhang ZC, Liang C, Wang Y, Xu RQ, Gao CF, Zhang CL. Static bending and vibration analysis of piezoelectric semiconductor beams considering surface effects. J Vibr Eng Technol. 2021;9:1789–800.